Italian Journal of Agrometeorology
Rivista Italiana di Agrometeorologia

Firenze University Press
www.fupress.com/ijam

OPEN ACCESS

Citation: Abdulqader Ibrahim, W., Gumus, V., & Seker, M. (2023). Investigating future projection of precipitation over Iraq using artificial neural network-based downscaling. *Italian Journal of Agrometeorology* (2): 79-94. doi: 10.36253/ijam-1929

Received: December 11, 2022

Accepted: October 6, 2023

Published: January 20, 2024

Data Availability Statement: All relevant data are within the paper and its Supporting Information files.

Competing Interests: The Author(s) declare(s) no conflict of interest.

ORCID:
WAI: 0000-0002-7210-6897
VG: 0000-0003-2321-9526
MS: 0000-0002-4007-0703

Author Statement:
WAI: Performing analysis, interpreting results, and writing the manuscript; VG: Conceptualization, coding, writing the manuscript; MS: Performing analysis, writing the manuscript and interpreting results.

Investigating future projection of precipitation over Iraq using artificial neural network-based downscaling

Wlat Abdulqader Ibrahim[1], Veysel Gumus[1,2,*], Mehmet Seker[1]

[1] *Department of Civil Engineering, Harran University, Sanliurfa 63050, Turkey*
[2] *Engineering Department, University of Durham, Durham, DH1 3LE, United Kingdom*
*Corresponding author. E-mail: gumus@harran.edu.tr

Abstract. Global climate change will affect the precipitation and the temperature, and its effects need to be investigated. General circulation models (GCM) are one of the most used approaches to assessing the future effects of climate change. However, different GCMs have been proposed by researchers, and their success in the regions needs to be tested. Therefore, in this study, the performance of 29 GCMs in predicting precipitation in the Iraq region for 102 stations is evaluated using the artificial neural network-based statistical downscaling method. In order to evaluate the performance of these models, Nash Sutcliffe Model Efficiency Coefficient (NSE), normalized root mean square error (nRMSE), Kling-Gupta Efficiency (KGE), The Modified Index of Agreement (md), and Comprehensive Rating Index (CRI) are used. A comparison of the results shows that NorESM1-ME, FGOALS-g2, and NorESM1-M models performed well in estimating the historical precipitation of the region, and NorESM1-ME had the best representation. As a final step, future precipitation changes in Iraq were analyzed spatially and temporally under the RCP4.5 and RCP8.5 scenarios.

Keywords: climate change, CMIP5, Iraq, precipitation, artificial neural network.

HIGHLIGHTS

- The performance of general circulation models (GCM) in predicting precipitation is evaluated in Iraq for 102 stations.
- The performance of 29 models is assessed via five different criteria
- The NorESM1-ME, FGOALS-g2, and NorESM1-M models performed well in estimating the historical precipitation of the region.
- Future precipitation changes in Iraq under different scenarios were evaluated temporally and spatially.

1. INTRODUCTION

Because of rapid human activities in industrial and economic development, land use change, and environmental degradation during the twentieth

century, greenhouse gases have increased in the atmosphere on the planet. Since the second half of the twentieth century, most parts of the world have experienced a temperature increase and climate change due to this increase (Chen and Sun 2013). Climate change significantly impacts natural ecosystems, one of the most significant consequences. It is these changes that have an impact on the number of products and services available from these resources and, ultimately, their benefits. As a result of climate change, the quality and quantity of water resources will be affected. In addition, the condition of forests and pastures, green space, wildlife, aquatic animals, etc. The impact of climate change on water resources is one of the main concerns of scientists from various fields. It is essential to study and monitor climate change, as it greatly impacts all human activities (Feng et al. 2010). In this context, the World Meteorological Organization (WMO) and the United Nations Environment Organization (UNEP), which were established in 1988 under the leadership of the Intergovernmental Panel on Climate Change (IPCC), have been tasked with conducting essential studies on climate researchers worldwide. Several reports have been published by this organization in order to determine the extent and impact of climate change. According to the IPCC's Fifth Assessment Report (AR5), the Earth's average temperature has increased by 0.6 degrees Celsius over the past century. Additionally, if greenhouse gas emissions do not decrease in the 21st century, average global temperatures will rise by 1.1 to 6.4 degrees Celsius (IPCC 2013).

The use of climate modelling is one of the critical steps in predicting the future trend of climate change and the measures to be taken based on these forecasts. A global climate model (GCM) predicts possible future climate changes. It is a numerical instrument that simulates the physical processes of the land surface, ocean, and atmosphere in regional and hydro climatological studies (Sreelatha and Anand Raj 2019). Researchers in different countries have developed GCM models in recent decades to understand and predict climate change (Her et al. 2019). As part of the coupled model intercomparison project (CMIP), these models are combined into a global project with a common comparative framework to improve knowledge of climate change (climate in the past and present, as well as improving the performance of climate models for different species) (Demirel and Moradkhani 2015). In recent years, a new generation of climate models, known as Earth models, have been developed in the context of phase 5 of the CMIP (CMIP5) global projects, which aim to reduce the uncertainty associated with the previous phase 3 of CMIP (CMIP3) (Eyring et al. 2016). Compared to their predecessors' CMIP3 models, the CMIP5 models have significantly improved climate simulation and forecasting (Wang et al. 2016). According to (Taylor et al. 2012), the performance of CMIP5 is due to the inclusion of more favorable climate simulations from the previous year. In the AR5 report, scenarios known as Representative Concentration Pathways (RCP) were used in the development of GCMs published under CMIP5. Based on the RCP scenarios developed by a scientific committee under the auspices of the IPCC in 2010, the main causes of climate change can be traced. These results can be applied to climate models. The results of these scenarios are used in climate models to calculate greenhouse gas concentrations and emissions. In the same meeting, the literature was reviewed regarding the characteristics determined, and four RCP types were defined for radiative forcing levels and routes. From smallest to largest, these radiative forcing scenarios are RCP2.6, RCP4.5, RCP6.0, and RCP8.5.

In several studies, the GCM published under CMIP5 has been used to investigate climate change's impact on meteorological parameters (Afzali-Gorouh et al. 2018; Shiravand and Dostkamiyan 2019). For example, Srinivasa Raju et al. (2016) evaluated India's maximum and minimum temperature simulation performance using 36 general atmospheric circulation models from CMIP5. Ruan et al. (2018) examined CMIP5 to evaluate the score-based method's effectiveness in predicting precipitation in China (Lower Mekong Basin). Elsaeed et al. (2021), the daily precipitation characteristics of the Zab River were examined using the (CMIP5) model from 1979 to 2005, and the future precipitation changes were predicted using RCP4.5 and RCP8.5.

Even though GCMs are decent tools in climate studies, they cannot be applied directly because their outputs are too coarse to explain local climate changes (Shiru et al. 2019; Noor et al. 2020). Climate change simulations based on GCMs cannot provide practical information about spatial scales below 200 kilometers. Therefore, it is necessary to downscale coarse-resolution GCM simulated climate variables such as precipitation to regional scales for more realistic simulations (Su et al. 2016). By applying downscaling methods, it is possible to convert the output of GCM models into reliable predictions of climate precipitation variables at a regional scale. Downscaling methods can be categorized into two groups: statistical and dynamic downscaling. Dynamic downscaling allows the climate scale to be reduced for an area bounded by the GCM models. A statistical downscaling approach equates large-scale climatic features to local climate data (Wilby and Wigley 1997). However, dynam-

ic downscaling, a method that relies on the complex physics of atmospheric processes, is both computationally expensive and time-consuming, requiring computers with high computing power and specialized personnel. On the other hand, the statistical downscaling method (SDSM) aims to find the relationship between the large-scale GCM outputs (predictors) and the climate variables at the basin scale (predictands) without providing any information about the physical area (Danandeh Mehr and Kahya 2016).

SDSM is based on establishing a relationship between predictors and predictands. However, many statistical downscaling methods are used in the literature. SDSMs are performed using either bias correction or regression methods, such as linear regression or machine learning. A significant advantage of bias correction methods is their simplicity and straightforward application. However, bias correction methods, such as the delta change approach, do possess limitations. Notably, they predominantly overlook variations in the temporal structure and variability of climate variables, including fluctuations in dry/wet spells or temperature (Maraun 2016). This is primarily because the delta change method assumes that biases are constant over time, and it does not consider changes in the distribution of climate parameters. Additionally, since bias correction methods use only the relevant GCM parameter as a predictor, other parameters are mostly ignored. In contrast, regression methods allow using different atmospheric variables in estimation (Seker and Gumus 2022). In this context, regression-based methods for statistical downscaling enable finding a relationship between the large-scale circulation variables of the GCM and the observed meteorological data. A particularly powerful tool in this regard is the Artificial Neural Network (ANN) regression method. It is capable of identifying complex relationships between predictors and basin-scale climate variables. The ANN method boasts distinct advantages over classical linear approaches, primarily its capacity to model intricate, non-linear relationships among multiple input and output variables. This ability is facilitated by the network's 'learning' nature, adapting its structure according to the data. Moreover, the ANN approach is robust against noise and offers considerable customization flexibility in terms of varying architectures, activation functions, and training algorithms (Nourani et al. 2013; Saraf and Regulwar 2016). This method in recent years have been mostly used in downscaling in different parts of the world. For example, Xu et al. (2020) used the ANN method to downscale GCMs in China's Upper Han River Basin, Rabezanahary Tanteliniaina et al. (2021) investigated the future impact of climate change on Africa (Mangoky River) using ANN techniques and soil and water assessment tool (SWAT) data. Seker and Gumus (2022) used ANN techniques for downscaling temperature and precipitation data in the Mediterranean region of Turkey.

Due to the differences in the ability of downscaled GCMs to simulate climate depending on the climatic zone, two methods have been used to select GCMs: past performance and envelope method (Srinivasa Raju et al. 2016; Salman et al. 2018; Iqbal et al. 2020). A GCM's past performance is mainly determined by its ability to reproduce the climate of the last few years and compare it with historical data (Wright et al. 2015). GCMs are generally chosen based on their ability to simulate past climates (Shiru et al. 2019; Iqbal et al. 2020; Khan et al. 2020), and it is generally accepted that if a GCM accurately simulates the past, it will also accurately simulate the future (Andrews et al. 2019).

The IPCC report (IPCC 2013) identifies North Africa and the Middle East region are particularly sensitive to climate change. The global average temperature changes much faster than in the Middle East and North Africa (Salman et al. 2018). Further, according to the World Meteorological Organization (WMO 2019), West Asia and the Middle East are experiencing one of the worst droughts and declining precipitation periods in human history. It is, therefore, imperative that climate change impacts precipitation, the primary source of water resources in these regions, to determine its impact.

The Middle East has been the subject of numerous studies over the past two decades on the impact of climate change on hydrological processes such as temperature, precipitation, and surface runoff. According to Zarenistanak (2018), precipitation might decrease under the RCP4.5 and RCP8.5 scenarios, according to most models under the Alborz Mountain area. Ostad-Ali-Askari et al. (2020) examined the prediction of future precipitation in Iran (Isfahan). Based on RCP4.5 results, a 17% decrease in precipitation is expected during winter. Also, RCP8.5 predicts 32.7% precipitation in the spring. According to RCP4.5 and RCP8.5, autumn had the lowest reduction in precipitation, 6.9% and 14.4%, respectively. Homsi et al. (2019) CMIP5 Precipitation predicted in Syria indicated precipitation decreased along the coast for all RCPs. A significant increase in precipitation (up to 76%) was observed in some areas in the northwest and southwest for RCPs 4.5 and 8.5. Precipitation decreased during the dry season, with the greatest reduction occurring in the coastal and northeast areas.

Regarding climate change, Iraq is an important region in the Middle East. Researchers have recently examined the effects of climate change on meteorological

parameters in this region since it is sensitive to climate change. For example, Al-Mukhtar and Qasim (2019) used the HadCM3 model to predict precipitation in Iraq using (SDSM) and the daily precipitation. The results indicated a decrease in precipitation for all months. According to Mohammed and Hassan (2022), the LARS_WG model was used to predict future precipitation in southern Iraq. CSIRO-Mk3.6.0, HadGEM2-ES, CanESM2, MIROC5, and NorESM1-M models were used to predict precipitation and temperature under RCP4.5 and RCP8.5 scenarios. The results indicated that each model shows a different rate of precipitation reduction. According to Hashim et al. (2022), Iraq's future precipitation and temperature prediction indicate that the southern and southwestern parts are the most affected. Based on the 20 CMIP5 models, Khayyun et al. (2020) examined the future precipitation for 35 stations in Iraq. Following the final ranking of these 20 CMIP5 models, only four were suitable for data projection scenarios, namely HadGEM2-AO, HadGEM2-ES, CSIRO-Mk36, and MIROC5.

It is seen that the projection studies carried out in Iraq are mostly regional or is made with a limited number of stations. Additionally, to the authors' knowledge, there is no study in Iraq that used the ANN method in downscaling for precipitation. In this study, future precipitation projections were made using SWAT data from 102 grid points in Iraq. For this purpose, The ANN-based SDSM method was used to determine the historical data estimation performances of 29 CMIP models. The most appropriate GCMs are selected based on five statistical performance criteria, NSE, nRMSE, KGE, and MD. Iraq's future precipitation projection between 2020 and 2100 was evaluated temporally and spatially based on two scenarios (RCP4.5 and RCP8.5).

2. STUDY AREA AND DATASETS

2.1. Study area and observed datasets

Iraq, situated in Southwest Asia, has geographical coordinates spanning from 29.25° N to 38.25° N in latitude and 38.75° E to 48.75° E in longitude. The Iraqi borderline is shared with Iran, Kuwait, Syria, Turkey, Jordan, and Saudi Arabia, as indicated in Figure 1a. The land area of Iraq is approximately 438,317 km2. Iraq is ranked 58th in the world in terms of land area. Geographically, Iraq is primarily lowland and tropical. There are deserts in the west, fertile plains in the east, and mountains in the northeast of Iraq. The minimum, maximum, and average annual precipitation were 63.18 millimeters, 1195.62 millimeters, and 216.1 millimeters, respectively. The mean, maximum, and minimum annual temperatures were 9.54 degrees Celsius, 26.79 degrees Celsius, and 22.61 degrees Celsius, respectively. As can be seen in Figure 1-b, the average yearly precipitation observed for all stations is shown. A dramatic decrease in precipitation is observed in Figure 1-b as it moves from north to south. A difference of up to 15 times between the region's lowest and highest precipitation indicates that precipitation is highly variable. Thus, a study that utilizes a small number of stations in Iraq, where precipitation varies, may not be reliable. In order to evaluate the projection, 102 stations in Iraq were uniformly distributed. Table 1 shows the number of stations and their provinces selected from Anbar province, which has the largest area, and Baghdad province, which has the smallest area. The data for the period 1979–2013 were obtained from the Global Weather Service (globalweather.tamu.edu).

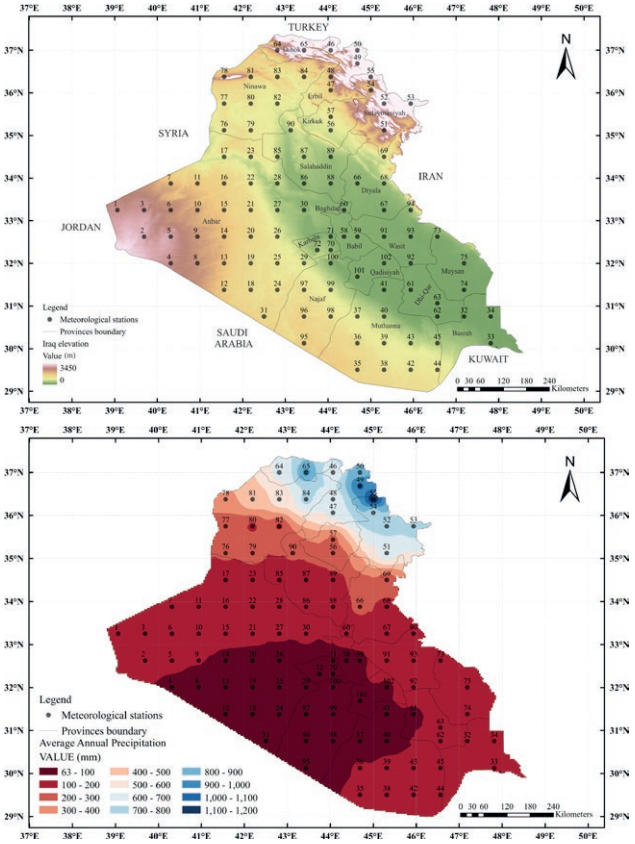

Figure 1. (a) Elevation map and location of the stations, (b) Spatial distribution of annual average precipitation (mm).

2.2. CMIP5 dataset

The GCMs are integral tools developed to simulate and predict large-scale climate dynamics for the past,

Table 1. The meteorological stations used in the study.

Province	No	Station ID	Province	No	Station ID	Province	No	Station ID
Anbar	1	333391	Muthanna	35	295447		69	345453
	2	326397		36	301447	Karbala	70	323441
	3	333397		37	308447		71	326441
	4	320403		38	295453		72	323438
	5	326403		39	301453	Maysan	73	326466
	6	333403		40	308453		74	314472
	7	339403		41	314453		75	320472
	8	320409		42	295459	Ninawa	76	351416
	9	326409		43	301459		77	358416
	10	333409		44	295466		78	364416
	11	339409		45	301466		79	351422
	12	314416	Erbil	46	370441		80	358422
	13	320416		47	361441		81	364422
	14	326416		48	364441		82	358428
	15	333416		49	367447		83	364428
	16	339416		50	370447		84	364434
	17	345416	Sulaymaniyah	51	351453	Salahaddin	85	345428
	18	314422		52	358453		86	339434
	19	320422		53	358459		87	345434
	20	326422		54	361450		88	339441
	21	333422		55	364450		89	345441
	22	339422	Kirkuk	56	351441		90	351431
	23	345422		57	354441	Wasit	91	326453
	24	314428	Babil	58	326444		92	320459
	25	320428		59	326447		93	326459
	26	326428	Baghdad	60	333444		94	333459
	27	333428	Dhi-Qar	61	314459	Najaf	95	301434
	28	339428		62	308466		96	308434
	29	320434		63	311466		97	314434
	30	333434	Dihok	64	370428		98	308441
	31	308425		65	370434		99	314441
Basrah	32	308472	Diyala	66	339447		100	320441
	33	301478		67	333453	Qadisiyah	101	317447
	34	308478		68	339453		102	320453

present, and future, providing an in-depth understanding of the Earth's complex climate system. However, their raw outputs are at a global scale. For local applications, these models need to be downscaled to capture regional climate variations. The effectiveness of these downscaled GCMs hinges on their ability to accurately reproduce the statistical characteristics of historical climate data on various timescales, from monthly to daily, in simulations of historical periods. Therefore, it's necessary to compare the downscaled simulated data with observational precipitation data during the historical period. This comparison allows us to evaluate the performance of the downscaled GCMs for analyzing and studying the impacts of climate change on local water resource systems.

A GCM data production server (www.dkrz.de) provided the climatic data required; the data obtained were for CMIP5. This first step involved extracting monthly data in NetCDF format for all climate variables obtained for 102 locations in the Iraq region. The process was carried out for 29 models of the CMIP5 (Table 2). CMIP5 models were used in this study for both single- and multiple-level data. In this study, monthly predicted time series of precipitation in the historical period of 1979-2005 have been used to compare with the corresponding historical time series at base stations. The inverse dis-

Table 2. The information of used CMIP5 models.

No	Model	Country	Resolution Lon° ×Lat°
1	ACCESS1.3	Australia	1.875° × 1.25°
2	BCC-CSM1.1	China	2.8125° × 2.7906°
3	BCC-CSM1.1(m)	China	2.8125° × 2.7906°
4	BNU-ESM	China	2.8125° × 2.7906°
5	CanESM2	Canada	2.8125° × 2.7906°
6	CCSM4	United States	1.25° × 0.9424°
7	CESM1-BGC	United States	1.25° × 0.9424°
8	CESM1-CAM5	United States	1.25° × 0.9424°
9	CESM1-WACCM	United States	2.5° × 1.8848°
10	CMCC-CM	Italy	0.75° × 0.7484°
11	CMCC-CMS	Italy	3.75° × 3.7111°
12	CNRM-CM5	United States	1.40625° × 1.4008°
13	CSIRO-Mk3-6-0	Australia	1.875° × 1.8653°
14	FGOALS-g2	China	2.8125° × 2.7906°
15	FIO-ESM	China	2.80° × 2.80°
16	GISS-E2-R	United States	2.5° × 2°
17	HadGEM2-AO	England	1.875° × 1.25°
18	INM-CM4	Russia	2° × 1.5°
19	IPSL-CM5A-LR	France	3.75° × 1.8947°
20	IPSL-CM5A-MR	France	2.5° × 1.2676°
21	IPSL-CM5B-LR	France	3.75° × 1.8947°
22	MIROC5	Japan	1.40625° × 1.4008°
23	MIROC-ESM	Japan	2.8125° × 2.7906°
24	MIROC-ESM-CHEM	Japan	2.8125° × 2.7906°
25	MPI-ESM-LR	Germany	1.875° × 1.8653°
26	MPI-ESM-MR	Germany	1.875° × 1.8653°
27	MRI-CGCM3	Japan	1.125° × 1.12148°
28	NorESM1-M	Norway	2.5° × 1.8947°
29	NorESM1-ME	Norway	2.5° × 1.8947°

tance weight averaging method was used to interpolate the predictors of GCMs with different resolutions from the four grid points closest to each station to bring them to the same resolution, and the obtained data were used as input in the ANN method.

3. METHOD

3.1. Procedure

The approach to this research is visualized in a sequence of steps detailed in Figure 2. It starts with data acquisition, where independent atmospheric variables from General Circulation Models (GCMs) are gathered for both a reference period (1979-2005) and a future period (December 2006-2100). The data is procured from the four closest GCM grid points to each station, utilizing the inverse distance interpolation method. Next in the process comes preprocessing and predictor selection. This step involves identifying the five GCM predictors that correlate most strongly with the historical temperature and precipitation data of each station. These predictors are subsequently defined as dominant. The dominant predictors serve as inputs in an ANN-based SDSM. Table 3 provides a list of all the predictors used in the study. This table outlines the predictors, all of which are aggregated on a monthly scale, along with their relevant units. The predictors include both multi-level variables such as relative humidity, and temperature for different geopotential height (200m, 300m, 500m and 850m), and single-level variables like sea level pressure, surface pressure, 2m temperature, and precipitation.

The aim of this model is to predict observed precipitation at each station. Performance evaluation follows, assessing the ability of the GCMs to simulate monthly total precipitation at the stations. This evaluation is based on five performance criteria: the Correlation Coefficient (CC), Nash-Sutcliffe Efficiency (NSE), normalized root mean square error (nRMSE), Kling-Gupta Efficiency (KGE), and Modified Agreement Index (md). In the model selection stage, the Comprehensive Rating Index (CRI) is used to identify the best-performing models based on the evaluation criteria. Finally, future projections for each station are made. These projections incorporate RCP4.5 and RCP8.5 scenarios for the period 2006-2100, using the top three best-performing GCMs.

The general procedure of this study is as follows:

1. First, the independent atmospheric variables of the GCM outputs (reference and future period) used in the ANN-based SDSM to generate for each station were obtained using the inverse distance interpolation method from the nearest four GCM grid points. The number of predictors was 16, including multi-level predictors such as geopotential height, relative humidity and temperature, as well as single-level predictors such as sea level pressure, surface pressure, 2m temperature and precipitation, with each multi-level predictor including five different levels: 200hpa, 300hpa, 500hpa and 850hpa. The data between 1979-2005 are evaluated as the reference period, and December 2006-2100 as the future period.
2. The first five GCMs predictors (out of 16) with the highest correlation with each station's historical temperature and precipitation data were selected as the dominant predictors.
3. The dominant predictors determined from the independent variables obtained from the GCMs were defined as inputs to the ANN-based model for pre-

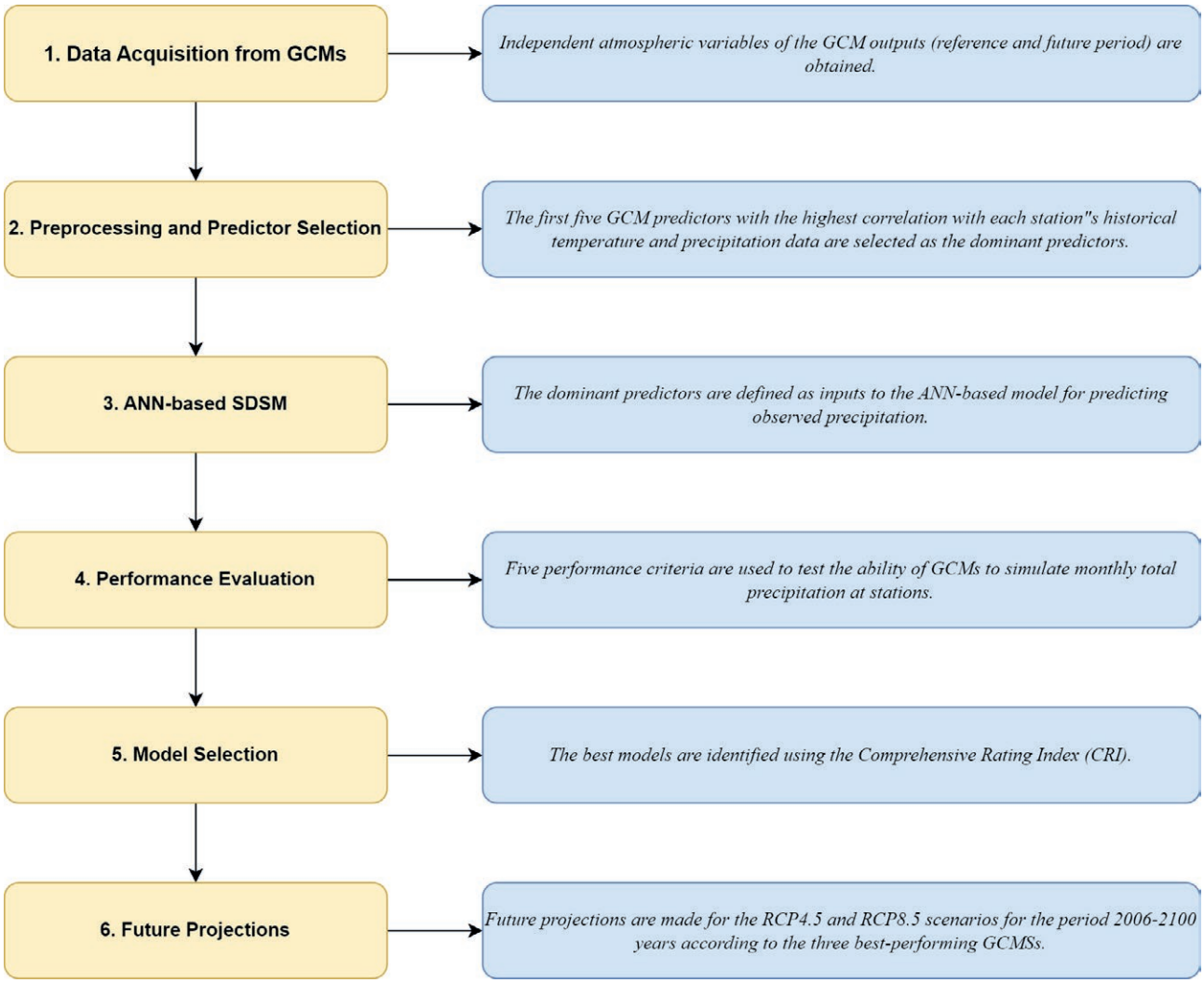

Figure 2. Flowchart of the study.

dicting observed precipitation. The observed precipitation data based on the station are defined as the model's output.

4. Five performance criteria are used to test the ability of GCMs to simulate monthly total precipitation at stations. These are Correlation Coefficient (CC), Nash-Sutcliffe Efficiency (NSE), normalized root mean square error (nRMSE), Kling-Gupta Efficiency (KGE) and Modified Agreement Index (md).
5. The best models in the study were identified using the Comprehensive Rating Index (CRI), which allows all performance criteria to be evaluated together.
6. Future projections from all regional synoptic stations for the RCP4.5 and RCP8.5 scenarios for the period 2006-2100 years were made according to the three best-performing GCMSs.

3.2. The artificial neural network method

The artificial neural network (ANN) method, particularly the feed-forward error backpropagation artificial neural network technique, is popular in hydrometeorology for modeling problems lacking analytical relationships (Seker and Gumus 2022). This study applies this technique to examine precipitation in Iraq, using 29 CMIP5 models across 102 stations. The ANN model consists of input, hidden, and output layers, with the model selecting five highly correlated independent variables with precipitation for each GCM model and station as an input. The output layer has a single value, and this is precipitation. The number of hidden layers is determined through a trial-and-error method, ranging from 1 to 10, with the optimal number yielding the low-

Table 3. List of used predictors.

Predictor variables	Units	Pressure level	Number of Variable
Air temperature	K	200,300,500 ,850	4
Air pressure at sea level	Pa	Sea level	1
Relative humidity	%	200,300,500 ,850	4
Jeopatential height	M	200,300,500 ,850	4
Near-surface temperature	K	Surface	1
Precipitation	Kg m^{-2} s^{-1}	Surface	1
Air pressure	Pa	Surface	1

est normalized root mean square error (nRMSE). Consequently, the study evaluates the performance of the GCMs in predicting precipitation and temperature in the Iraq region by generating 2958 models, derived from the 29 models, 102 stations. The detail of the method can be found in Keskin and Terzi (2006)

3.3. Assessment of the GCM models

In order to determine the success of the downscaled GCMs in predicting precipitation observed with ANN-based models, four quantitative performance evaluation criteria were applied. As explained in Equations 1-4, these are Nash coefficients (NSE), normalized root mean square errors (nRMSE), Kling-Gupta efficiency (KGE), and The Modified Index of Agreement (md) (McMahon et al. 2015). As a result, the most successful method of model determination has been The Comprehensive Rating Index (CRI) method (Equation 5), which allows for ranking among the models by making a joint evaluation of all methods involved. Among these coefficients, NSE, KGE, and md are close to 1, and md to zero indicates that the model's success has increased. A CRI value of 1 indicates that a model is most successful.

$$\mathrm{NSE} = 1 - \left(\frac{\sum_{i=1}^{N}(P_{sml,i} - P_{obs,i})^2}{\sum_{i=1}^{N}(P_{obs,i} - \overline{P}_{obs})^2}\right) \quad (1)$$

$$NRMSE = \frac{\sqrt{\frac{1}{N}\sum_{i=1}^{N}(P_{sml,i} - o_{obs,i})^2}}{P_{obs(\max)} - P_{obs(\min)}} \quad (2)$$

$$KGE = 1 - \sqrt{(CC-1)^2 + \left(\frac{\overline{P_{sml}}}{P_{obs}} - 1\right)^2 + \left(\frac{\sigma_{model}/\overline{P_{sml}}}{\sigma_{obs}/\overline{P_{obs}}} - 1\right)^2} \quad (3)$$

$$md = 1 - \frac{\sum_{i=1}^{N}\left|P_{obs,i} - P_{sml,i}\right|}{\sum_{i=1}^{N}\left(\left|P_{sml,i} - \overline{P_{obs}}\right| + \left|P_{obs,i} - \overline{P_{obs}}\right|\right)} \quad (4)$$

$$CRI = 1 - \frac{1}{nm}\sum_{i=1}^{n} Rank_i \quad (5)$$

Where, $P_{obs,i}$ and are the observed and simulated values, respectively, $\overline{P_{obs}}$ and $\overline{P_{sml}}$ are the average observed and simulated values, respectively, and N is the number of data

4. RESULTS

4.1. Performance evaluation of GCMs

A compatibility analysis is conducted between the observed total precipitation data from 1979-2005 in the Iraq region and the predicted precipitation data derived from the CMIP5 model. Based on four statistical performance criteria, Figure 3 evaluates the predicted and observed precipitation values using 29 different GCMs of the CMIP5 model. These results indicate that the success of the models varies depending on the criteria. For example, a successful model is found to be FGOALS-g2 based on the NSE, KGE, and nRMSE values, whereas NorESM1-ME is successful based on the MD value. Due to this, it would be more realistic to determine the most successful models based on the CRI value, which evaluates the model performance by considering all criteria. The distribution of the calculated CRI values for each of the models used is shown in Figure 4. Further, Figure 5 shows the ranking of each model based on the CRI values. Therefore, nine GCM models have an acceptable CRI value (CRI>0.5). Furthermore, two of these models have an average CRI value above 0.6. These models are NorESM1-ME and FGOALS-g2.

The numbers in the heat map represent the rank of models. For example, the most successful model rank value in this is 1, while the worst is 29. The CRI results show that the NorESM1-ME, FGOALS-g2, and NorESM1-M models generally perform well in estimating the historical precipitation of the region. Figure 5 shows that NorESM1-ME is the most accurate model according to average ranks. This model was the most successful at 15 stations and among the top five most successful models at 57 stations.

On the other hand, the FGOALS-g2 model was the most accurate at more stations (17 stations) than the NorESM1-ME model. However, this model was among the top five most successful models at 44 stations. In addition, the third-best model, NorESM1-M, was the most successful model at only four stations and was among the list of the five most successful models at 29 stations. While the NorESM1-ME model can be considered the best-representing model for Iraq in general, it

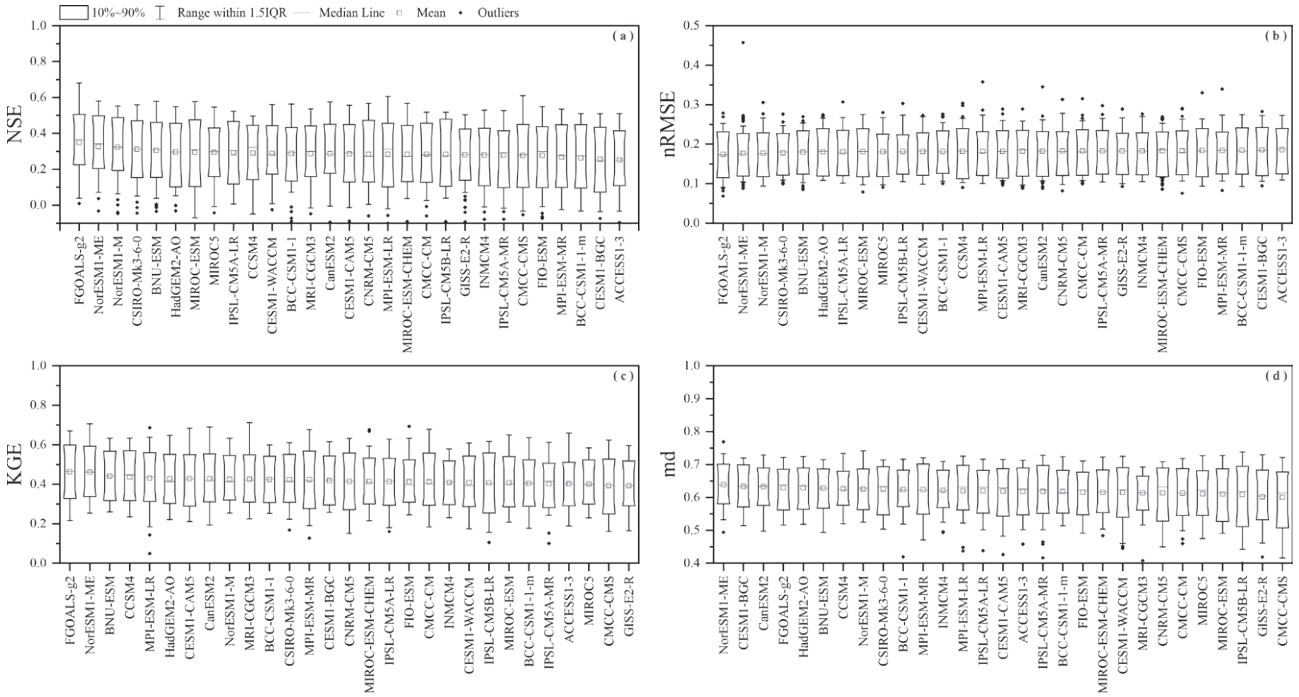

Figure 3. The distribution of statistics parameters (a) Nash coefficient, (b) nRMSE, (c) KGE, (d) md.

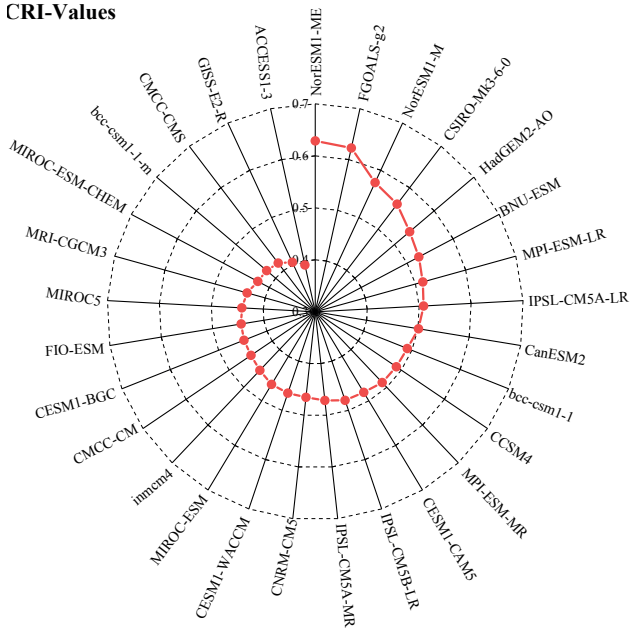

Figure 4. The radar graph of CRI values for all used CMIP5 models.

has been observed to be ineffective only at the stations located in the mountainous regions in the north. Mostly, the FGOALS-g2 and NorESM1-M models performed well at these stations. Therefore, the future projection of the region for two scenarios (RCP4.5 and RCP8.5) was evaluated with these three models.

4.2. Projection of precipitations for RCP4.5 scenario

In this part of the study, future precipitation projections for the Iraq region are based on the outputs of the best-performing GCMs in simulating historical precipitation. According to Figure 6, the average monthly precipitation in the future period (2006-2100) is different from the observation period (1979-2005) for the NorESM1-ME, FGOALS-g2, and NorESM1-M models with the RCP4.5 scenarios. According to RCP4.5, the seasonal precipitation for Iraq stations will decrease in all seasons. According to NorESM1-ME, FGOaLS-g2, and NOrESM1-M, the average seasonal decrease in spring was 20.37%, 20.49%, and 18%, respectively. 22.5%, 11.66%, and 16.67% were recorded for the autumn. However, the winter season was 5.56%, 6.33% and 5.68%. According to all models, the maximum decrease occurs during the spring season.

Based on historical precipitation, Figure 7 illustrates the spatial distribution of station-based changes in Iraq for the three most appropriate CMIP5 models. According to the results of the NorESM1-ME model, which gave successful results in the southern regions, the maximum decreases were -63%, -84.93%, -64.01%

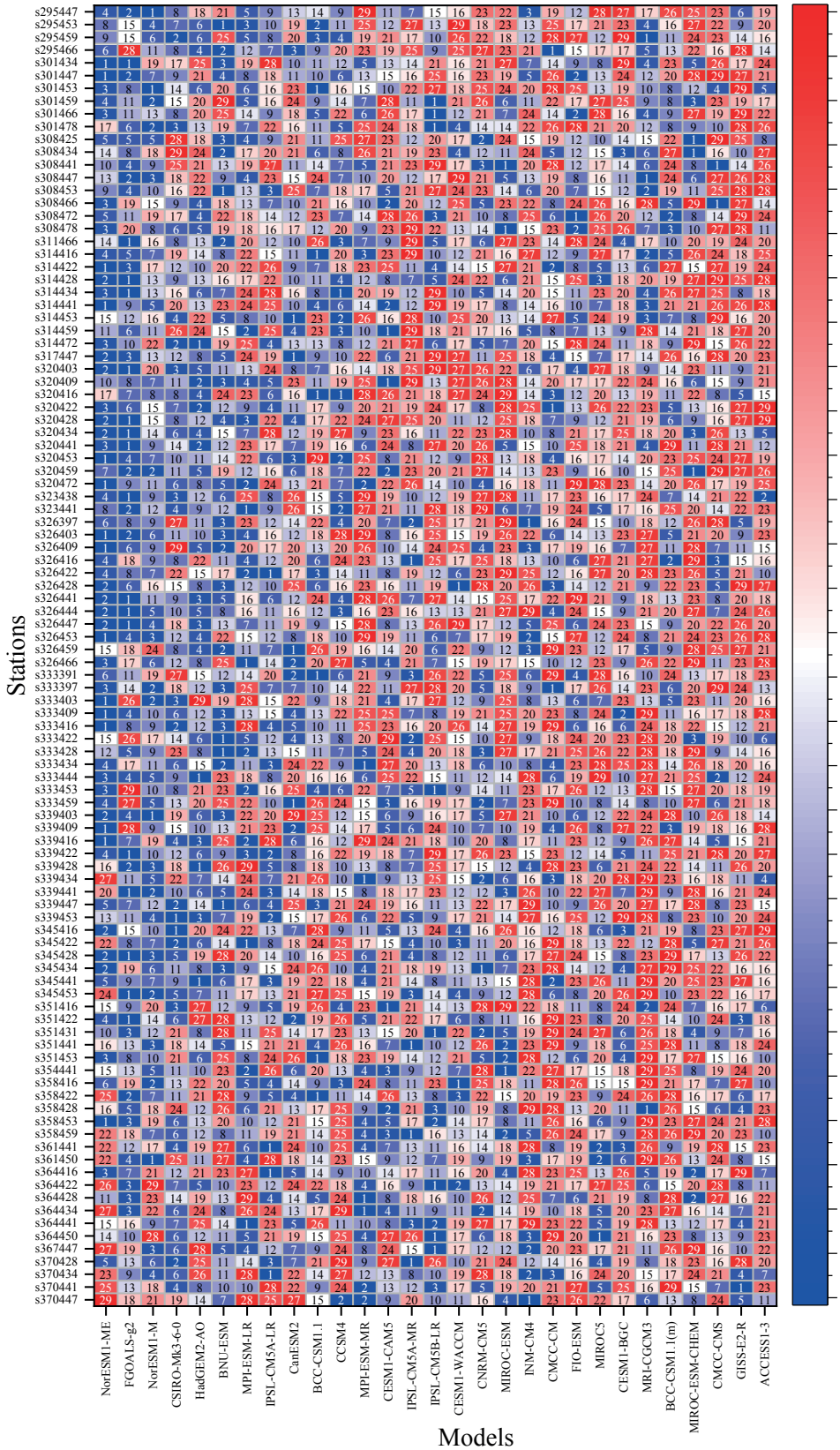

Figure 5. The heat map of 29 CMIP models based on the CRI ranking.

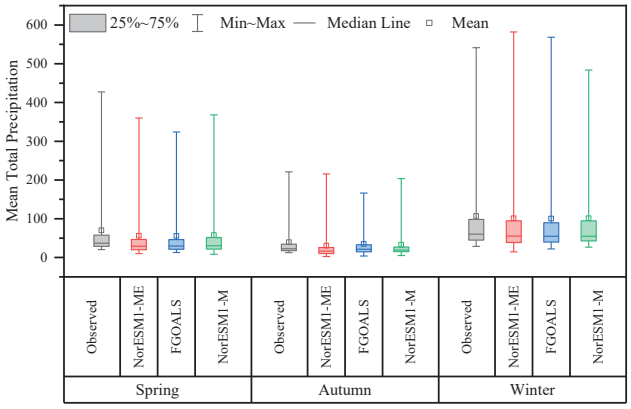

Figure 6. The box plot of observed and future precipitation for seasons according to the RCP4.5 scenario.

for spring, autumn, and winter, respectively. While the highest percentage of the decrease occurred in the autumn in the southern region, it is noteworthy that an increase occurred in the spring and winter in the mountainous northern regions. Additionally, spring precipitation was slightly increased in the eastern partially desert region. However, in the previous section, it was stated that NorESM1-ME did not produce successful results in northern regions. Therefore, to evaluate the future projections for the northern regions, spatial maps of the changes based on FGOALS-g2 and NorESM1-M, two successful models, are shown in Figures 7 (b) and (c). This map indicates that precipitation will increase significantly in the northern region during the spring and winter but decrease in the autumn months.

4.3. Projection of precipitations for RCP8.5 scenario

Based on the RCP8.5 scenario, future seasonal precipitation for Iraq stations will decrease in all seasons' average precipitation (Figure 8). According to NorESM1-ME, FGOaLS-g2 and NOrESM1-M, the average seasonal decreases were 33.52%, 36.69%, and 28.06%, respectively, in the spring season. The autumn season represented 29.93%, 29.41%, and 24.30%, whereas the winter season represented 11.76%, 15.16%, and 12.06%. Therefore, the maximum decrease is observed to be associated with the spring season, as indicated by all models. In this scenario, precipitation decreased more than in RCP4.5, as expected.

Based on the RCP8.5 scenario, Figure 9 shows the spatial distributions of the station-based changes in Iraq according to historical precipitation using the three most accurate CMIP5 models. The spatial distribution of precipitation changes for the most accurate model, NorESM1-ME, is shown in Figure 9 (a). This model determined that the maximum decreases could be as high as -71.39% in spring, -84.54% in autumn, and -77.57% in winter, respectively. Precipitation increases in the region's east relative to RCP4.5 in spring were not observed in this scenario. On the contrary, the decrease in precipitation is seen at almost all stations except the northern region in spring. In autumn and winter, all regions except a few stations in the middle and south regions follow this. Therefore, when the FGOALS-g2 and NorESM1-M model results for the northern regions are evaluated, it is understood that there is an increase in the north only in spring, but a decrease in precipitation will occur in the northern regions in other seasons.

5. DISCUSSION

Climate change projections for historical (1979-2005) and future (2006-2100) time periods were made for 102 stations with 29 GCM outputs published in CMIP5 for the Iraq region. In the study, the ability of the models to simulate historical data was evaluated, and future projections were made based on the three most successful GCMs. According to the results of the present study, NorESM1-ME, FGOALS-g2, and NorESM-M ranked the first three based on the CRI value, a common evaluation criterion for the ability of GCMs to simulate historical data. It is observed that the models have an acceptable ability to predict precipitation in the region with moderate to low accuracy. It was also found that although the models provide reliable precipitation predictions, they have weak prediction capabilities in some cases. In the study conducted by Abbas et al. (2022) to simulate the historical precipitation data of CMIP5 models with bias correction method over the Iraqi region, it is seen that the success of NorESM1-ME and NorESM1-M models is not parallel. In the studies conducted by Homsi et al. (2019) in Syria and Abbasian et al. (2018) in Iran, which are neighbouring border countries with similar climatic conditions, the ability of the NorESM1-M model to simulate historical precipitation data is at a good level, which supports the findings of the present study.

Although the precipitation in the region in this study changes partially from model to model, it is seen that, on average, there is a general decrease in all models. It is noted that the change in precipitation is greater in the RCP8.5 scenario compared to the RCP4.5 scenario. It can be seen that the decreases in the southern parts of the region are more pronounced than in the northern parts. For example, in the projection study carried out by Mohammed and Hassan (2022) in a local region

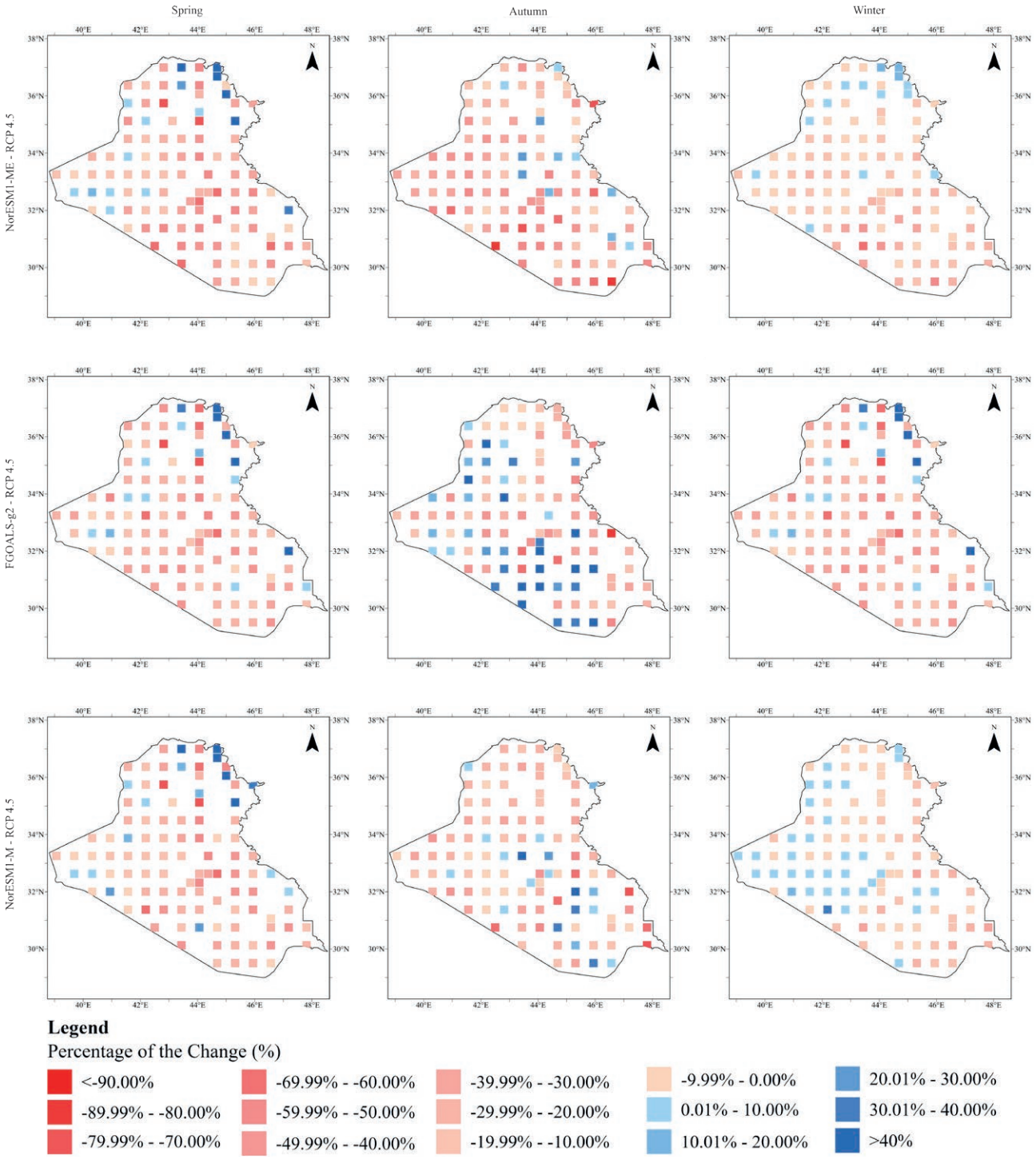

Figure 7. Spatial distribution of percentage change of the precipitation according to the RCP4.5 scenario for NorESM1-ME, FGOALS-g2 and NorESM1-M.

in south-eastern Iraq using the LARS-WG6.0 statistical scale reduction method, it was found that precipitation during the rainy seasons (autumn, winter, and spring) will increase in the future. In another study conducted by Al-Mukhtar and Qasim (2019), it was stated that precipitation in the region would decrease more in the

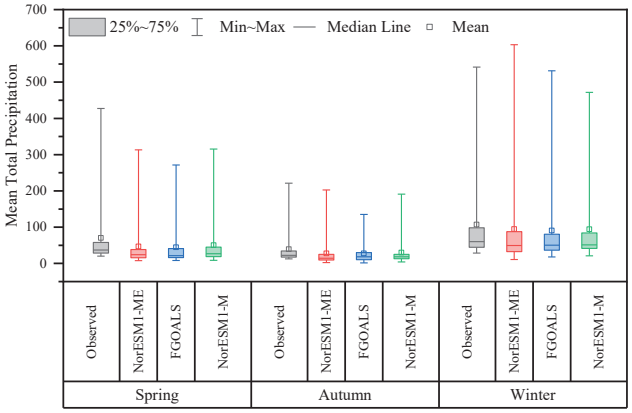

Figure 8. The box plot of observed and future precipitation for seasons according to the RCP8.5 scenario.

northern than in the southern parts using the statistical scale reduction method. In another study, Hamed et al. (2022) stated that precipitation will decrease in the northern parts of the region and increase in the southern regions. The results of this study are not in parallel with the above study. In addition, the results obtained in the study conducted in the southern parts of Khuzestan province (Rahimi et al. 2019), which is located in the southern parts of Khuzestan province within the borders of Iran, a regional neighbour, show that precipitation will decrease in the rainy seasons in the future; this result is in line with this study.

The assessment of the future seasonal precipitation change in the region shows an increase, especially in winter and spring months and a decrease in autumn months in the southern regions according to the RCP4.5 scenario. Considering the precipitation change in the region, the decreases in the spring months are significant. Considering the RCP8.5 scenario assessment, although it is more significant than the RCP4.5 scenario, the decrease in spring precipitation is also generally significant. In the study conducted by Ozturk et al. (2018), there is a decrease in precipitation in all seasons in the region in general. In another study conducted by Evans (2008), it is observed that there is an increase in precipitation in all seasons, and the increases are significant, especially in the autumn months.

6. CONCLUSION

In this study, the most successful CMIP5 model for the future projection of precipitation values of 102 stations in Iraq was determined using five different statistical parameters. While the model that best represents the country, in general, was the NorESM1-ME model, this model was insufficient to represent the country's northern region. Therefore, the most successful 2nd and 3rd Models in the country's northern region were FGOALS-g2 and NorESM1-M. In addition, the future projection of the country was evaluated according to two different scenarios using the most successful models. As a result of the projection study carried out according to RCP4.5, it was determined that the precipitation would decrease in the majority of the country, and there is a potential for a decrease in precipitation only in the northern region of the country in some seasons. On the other hand, according to RCP8.5, it has been seen that there will be a severe decrease in precipitation in almost the whole country.

Precipitation may decrease in regions sensitive to climate change, such as Iraq, and regions already suffering from drought will experience more problems. For this reason, it is considered that it will be helpful to examine the change in precipitation by the projection of precipitation and temperature with CMIP6 in addition to CMIP5 in Iraq by using soft computing techniques in downscaling.

REFERENCES

Abbas SA, Xuan Y, Al-Rammahi AH, Addab HF. 2022. A Comparison Study of Observed and the CMIP5 Modelled Precipitation over Iraq 1941–2005. Atmosphere. 13(11).

Abbasian M, Moghim S, Abrishamchi A. 2018. Performance of the general circulation models in simulating temperature and precipitation over Iran. Theoretical and Applied Climatology. 135(3-4): 1465-1483.

Afzali-Gorouh Z, Bakhtiari B, Qaderi K. 2018. Probable maximum precipitation estimation in a humid climate. Natural Hazards and Earth System Sciences. 18(11): 3109-3119.

Al-Mukhtar M, Qasim M. 2019. Future predictions of precipitation and temperature in Iraq using the statistical downscaling model. Arabian Journal of Geosciences. 12(2).

Andrews T, Andrews MB, Bodas-Salcedo A, Jones GS, Kuhlbrodt T, Manners J, Menary MB, Ridley J, Ringer MA, Sellar AA et al. 2019. Forcings, Feedbacks, and Climate Sensitivity in HadGEM3-GC3.1 and UKESM1. Journal of Advances in Modeling Earth Systems. 11(12): 4377-4394.

Chen H, Sun J. 2013. Projected change in East Asian summer monsoon precipitation under RCP scenario. Meteorology and Atmospheric Physics. 121(1-2): 55-77.

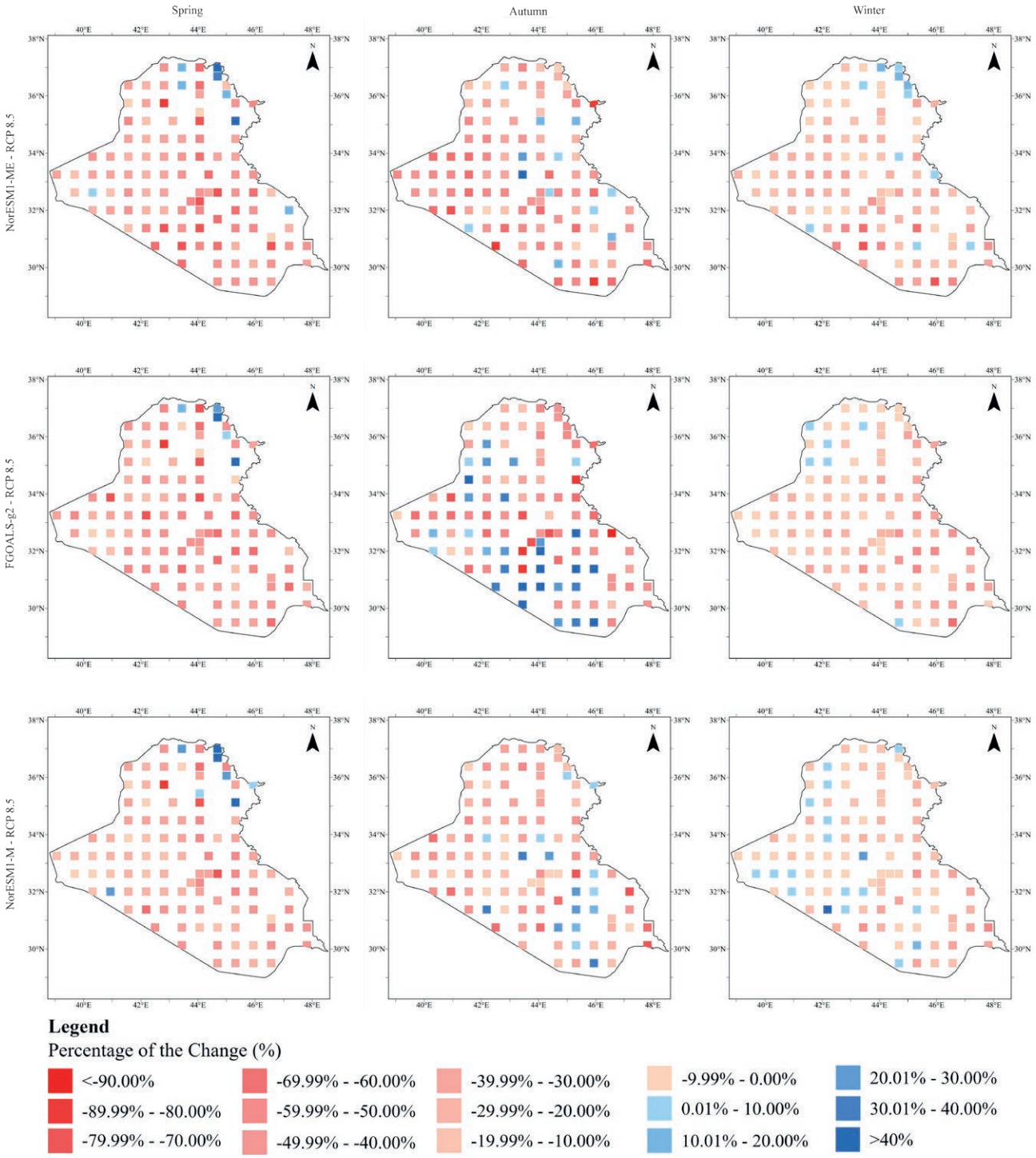

Figure 9. Spatial distribution of percentage change of the precipitation according to the RCP8.5 scenario for NorESM1-ME, FGOALS-g2 and NorESM1-M.

Danandeh Mehr A, Kahya E. 2016. Grid-based performance evaluation of GCM-RCM combinations for rainfall reproduction. Theoretical and Applied Climatology. 129(1-2): 47-57.

Demirel MC, Moradkhani H. 2015. Assessing the impact of CMIP5 climate multi-modeling on estimating the precipitation seasonality and timing. Climatic Change. 135(2): 357-372.

Elsaeed GH, Kheireldin K, AL-Sheer MT, Elzahry EF. 2021. Long Term Impact of Climate Change on Precipitation of Greater Zab River Basin, Iraq. Engineering Research Journal. 1(47): 130-138.

Evans JP. 2008. 21st century climate change in the Middle East. Climatic Change. 92(3-4): 417-432.

Eyring V, Bony S, Meehl GA, Senior CA, Stevens B, Stouffer RJ, Taylor KE. 2016. Overview of the Coupled Model Intercomparison Project Phase 6 (CMIP6) experimental design and organization. Geoscientific Model Development. 9(5): 1937-1958.

Feng J, Wang L, Chen W, Fong SK, Leong KC. 2010. Different impacts of two types of Pacific Ocean warming on Southeast Asian rainfall during boreal winter. Journal of Geophysical Research: Atmospheres. 115(D24).

Hamed MM, Nashwan MS, Shiru MS, Shahid S. 2022. Comparison between CMIP5 and CMIP6 Models over MENA Region Using Historical Simulations and Future Projections. Sustainability. 14(16).

Hashim BM, Al Maliki A, Alraheem EA, Al-Janabi AMS, Halder B, Yaseen ZM. 2022. Temperature and precipitation trend analysis of the Iraq Region under SRES scenarios during the twenty-first century. Theoretical and Applied Climatology. 148(3-4): 881-898.

Her Y, Yoo S-H, Cho J, Hwang S, Jeong J, Seong C. 2019. Uncertainty in hydrological analysis of climate change: multi-parameter vs. multi-GCM ensemble predictions. Scientific Reports. 9(1).

Homsi R, Shiru MS, Shahid S, Ismail T, Harun SB, Al-Ansari N, Chau K-W, Yaseen ZM. 2019. Precipitation projection using a CMIP5 GCM ensemble model: a regional investigation of Syria. Engineering Applications of Computational Fluid Mechanics. 14(1): 90-106.

IPCC A. 2013. Climate change 2013: the physical science basis. Contribution of working group I to the fifth assessment report of the intergovernmental panel on climate change. 1535.

Iqbal Z, Shahid S, Ahmed K, Ismail T, Khan N, Virk ZT, Johar W. 2020. Evaluation of global climate models for precipitation projection in sub-Himalaya region of Pakistan. Atmospheric Research. 245.

Keskin ME, Terzi Ö. 2006. Artificial Neural Network Models of Daily Pan Evaporation. Journal of Hydrologic Engineering. 11(1): 65-70.

Khan JU, Islam A, Das MK, Mohammed K, Bala SK, Islam G. 2020. Future changes in meteorological drought characteristics over Bangladesh projected by the CMIP5 multi-model ensemble. Climatic Change. 162(2): 667-685.

Khayyun TS, Alwan IA, Hayder AM. 2020. Selection of Suitable Precipitation CMIP-5 Sets of GCMs for Iraq Using a Symmetrical Uncertainty Filter. IOP Conference Series: Materials Science and Engineering. 671(1).

Maraun D. 2016. Bias Correcting Climate Change Simulations - a Critical Review. Current Climate Change Reports. 2(4): 211-220.

McMahon TA, Peel MC, Karoly DJ. 2015. Assessment of precipitation and temperature data from CMIP3 global climate models for hydrologic simulation. Hydrology and Earth System Sciences. 19(1): 361-377.

Mohammed ZM, Hassan WH. 2022. Climate change and the projection of future temperature and precipitation in southern Iraq using a LARS-WG model. Modeling Earth Systems and Environment.

Noor M, Ismail Tb, Ullah S, Iqbal Z, Nawaz N, Ahmed K. 2020. A non-local model output statistics approach for the downscaling of CMIP5 GCMs for the projection of rainfall in Peninsular Malaysia. Journal of Water and Climate Change. 11(4): 944-955.

Nourani V, Baghanam AH, Adamowski J, Gebremichael M. 2013. Using self-organizing maps and wavelet transforms for space–time pre-processing of satellite precipitation and runoff data in neural network based rainfall–runoff modeling. Journal of Hydrology. 476: 228-243.

Ostad-Ali-Askari K, Ghorbanizadeh Kharazi H, Shayannejad M, Zareian MJ. 2020. Effect of climate change on precipitation patterns in an arid region using GCM models: case study of Isfahan-Borkhar Plain. Natural Hazards Review. 21(2): 04020006.

Ozturk T, Turp MT, Türkeş M, Kurnaz ML. 2018. Future projections of temperature and precipitation climatology for CORDEX-MENA domain using RegCM4.4. Atmospheric Research. 206: 87-107.

Rabezanahary Tanteliniaina MF, Rahaman MH, Zhai J. 2021. Assessment of the Future Impact of Climate Change on the Hydrology of the Mangoky River, Madagascar Using ANN and SWAT. Water. 13(9).

Rahimi A, Borna R, Morshedi J, Ghorbanian J. 2019. The Vulnerability of Infrastructure of the Southern Regions of Khuzestan Province in Climate Change Conditions. Environmental Management Hazards. 6(4): 361-376.

Salman SA, Shahid S, Ismail T, Ahmed K, Wang X-J. 2018. Selection of climate models for projection of spatiotemporal changes in temperature of Iraq with uncertainties. Atmospheric Research. 213: 509-522.

Saraf VR, Regulwar DG. 2016. Assessment of Climate Change for Precipitation and Temperature Using Statistical Downscaling Methods in Upper Godavari River Basin, India. Journal of Water Resource and Protection. 8(1): 31-45.

Seker M, Gumus V. 2022. Projection of temperature and precipitation in the Mediterranean region through multi-model ensemble from CMIP6. Atmospheric Research. 280.

Shiravand H, Dostkamiyan M. 2019. Analysis of Temperature Fluctuations in the South West of Iran Based on General Circulation Model and Neural Network (Case Study: Plain and Mountainous Stations). Iran-Water Resources Research. 15(3): 206-217.

Shiru MS, Shahid S, Chung E-S, Alias N, Scherer L. 2019. A MCDM-based framework for selection of general circulation models and projection of spatio-temporal rainfall changes: A case study of Nigeria. Atmospheric Research. 225: 1-16.

Sreelatha K, Anand Raj P. 2019. Ranking of CMIP5-based global climate models using standard performance metrics for Telangana region in the southern part of India. ISH Journal of Hydraulic Engineering. 27(supl): 556-565.

Srinivasa Raju K, Sonali P, Nagesh Kumar D. 2016. Ranking of CMIP5-based global climate models for India using compromise programming. Theoretical and Applied Climatology. 128(3-4): 563-574.

Su B, Huang J, Gemmer M, Jian D, Tao H, Jiang T, Zhao C. 2016. Statistical downscaling of CMIP5 multi-model ensemble for projected changes of climate in the Indus River Basin. Atmospheric Research. 178-179: 138-149.

Taylor KE, Stouffer RJ, Meehl GA. 2012. An Overview of CMIP5 and the Experiment Design. Bulletin of the American Meteorological Society. 93(4): 485-498.

Wang X, Yang T, Li X, Shi P, Zhou X. 2016. Spatio-temporal changes of precipitation and temperature over the Pearl River basin based on CMIP5 multi-model ensemble. Stochastic Environmental Research and Risk Assessment. 31(5): 1077-1089.

Wilby RL, Wigley TM. 1997. Downscaling general circulation model output: a review of methods and limitations. Progress in physical geography. 21(4):530-548.

WMO. 2019. Greenhouse gas concentrations, in atmosphere reach yet another high. Geneva, Switzerland: World Meteorological Organization (WMO).

Wright DB, Knutson TR, Smith JA. 2015. Regional climate model projections of rainfall from U.S. landfalling tropical cyclones. Climate Dynamics. 45(11-12): 3365-3379.

Xu R, Chen N, Chen Y, Chen Z. 2020. Downscaling and Projection of Multi-CMIP5 Precipitation Using Machine Learning Methods in the Upper Han River Basin. Advances in Meteorology. 2020: 1-17.

Zarenistanak M. 2018. Historical trend analysis and future projections of precipitation from CMIP5 models in the Alborz mountain area, Iran. Meteorology and Atmospheric Physics. 131(5): 1259-1280.